GEM TN-93-413
MIT-GEM-EM-018

Thermoelectrical Analyses of the GEM Detector Thermosiphon

A. L. Radovinsky
Plasma Fusion Center
Massachusetts Institute of Technology

May 17, 1993

Abstract:

Joule heating of GEM detector magnet bobbins was analyzed in [1] without considering effects due to the presence of the thermosiphon cooling tubes. Later the tubing was introduced [2] into the analysis in the form of jumpers connecting the bobbin quadrants; the results showed that the impact of the tubing was small. This memo presents the results of the electromagnetic analyses for the thermosiphon cooling tubes and peripherals considered as a curcuit including the manifolds and the cooling tubes (one per quadrant) as well as the bobbin quadrants. The results show that the maximum heating of the most sensitive elements is small.

MIT-GEM-EM-018

Thermoelectrical Analyses of the GEM Detector Thermosiphon

17 May 1993

A. L. Radovinsky

This document and all reports and memoranda in this series are intended as a record of MIT work in progress. They are for use in informal discussions of design and fabrication alternatives. This material is subject to change and should not, therefore, be published or referred to in the open literature. Conclusions are preliminary and distribution should be strictly limited.

Plasma Fusion Center
Massachusetts Institute of Technology
Cambridge, MA 02139

MIT GEM Detector Memoranda
Approval Sheet

B.A. Smith
Project Engineer

5/18/93
Date

R.D. Pillsbury, Jr.
Technical Monitor

5/18/93
Date

A.M. Dawson
Technical Editor

19 May 93
Date

ABSTRACT

The Joule heating of GEM detector magnet bobbins was analyzed and results obtained without considering effects due to the presence of the thermosiphon cooling tubes and with the tubing modeled as jumpers connecting the bobbin quadrants were presented in memoranda MIT-GEM-EM-014 and MIT-GEM-EM-016. This memo presents the results of the electromagnetic analyses for the thermosiphon cooling tubes and peripherals considered as a circuit including the manifolds and the cooling tubes as well as the bobbin quadrants. The results show that the maximum heating of the most sensitive elements is small.

ABSTRACT

Joule heating of GEM detector magnet bobbins was analyzed in [1] without considering effects due to the presence of the thermosiphon cooling tubes. Later the tubing was introduced [2] into the analysis in the form of jumpers connecting the bobbin quadrants; the results showed that the impact of the tubing was small. This memo presents the results of the electromagnetic analyses for the thermosiphon cooling tubes and peripherals considered as a circuit including the manifolds and the cooling tubes (one per quadrant) as well as the bobbin quadrants. The results show that the maximum heating of the most sensitive elements is small.

ANALYSIS

The dimensions of the model are shown in Fig. 1. An axial cross section of a set of 12 cylindrical coil modules and thin conducting bobbins is shown, with axial symmetry about the Z-axis and a plane of symmetry at Z=0.

The coils were modeled as uniform current density solenoids with a centroid radius of 9.5 m, thickness of 0.02 m, and length in Z-direction of 0.9709 m. The current (I) in all solenoids is the same, corresponding to discharge, with an exponential current decay characterized by a time constant of 100 s. That is

$$I=950*\exp(-t/100) \quad kA$$

The thermosiphon diagram is shown on Fig. 2. Figure 3 displays a diagram of a passive circuit modelling the thermosiphon with integrated bobbin walls. The system is considered in a resistive approximation, neglecting the inductive coupling of any one conductor to the others. In the case under consideration, such an assumption is conservative and gives an upper limit of the power losses.

The circuits consist of 11 pairs of current loops formed by supply and return manifolds, each connected at even spaces by 12 jumpers made up of bobbin quadrants linked by tubing jumpers.

Table 1 shows the data concerning the resistances of the elements of the circuit:

a. A quadrant of 1.875 m width, 0.076 m thickness, and length corresponding to a quarter of the circumference at a radius of 9.582 m. The cross sections of the quadrants also include the cross sections of two flanges, 0.026 m^2 each.

b. Tubing jumpers connecting the quadrants to each other (0.0508 m long, 0.0254 OD, 0.002413 m wall thickness).

c. Tubing jumpers connecting the quadrants to the manifolds (same as b.)

d. Sections of the manifolds between the points of branching (1.875 m long, 0.1016 OD, 0.0060198 m wall).

To obtain the flux, Φ, in the loops, the radial component of the magnetic field, B_r, due to the coil currents at the initial time point t=0 at radius of 9.582 m was calculated using the program EDDYCUFF [2]. The chart of B_r versus Z is shown in Fig. 4.

Table 2 shows the results of the analyses. It consists of two parts. In the first part of Table 2 the data for current loops are displayed:

* The average of B_r over the corresponding loop;
* $d\Phi/dt$ at t=0 calculated as the average of Br multiplied by the area of the loop and divided by the time constant;
* The current in each of the loops calculated using the lumped parameter circuit equations ignoring inductive effects;
* Current density in the sections of the supply manifolds of the corresponding loops (currents in the return manifolds are equal to zero due to symmetry);
* Rise of temperature in sections of the supply manifolds based on the heat transfer coefficient h=3 kW/m^2/K. This is the steady state temperature rise across the tube wall assuming the maximum eddy currents induced at time t=0 are thereafter constant.

The second part of Table 2 displays currents in the bobbins, as well as current densities and temperature increases in the tubing jumpers (b and c), based on the same assumptions as described above.

RESULTS

Table 2 shows that temperature increases in the tubing jumpers are small. The maximum dT=0.006 K takes place in the 12th bobbin which is first from the edge of the magnet. It is a part of the 11th loop which is under the influence of the maximum radial magnet flux. In addition, this bobbin does not carry return currents from the next loop as all the other bobbins except for the first one do.

The values of dT in the supply manifolds are larger than in the tubing jumpers, but are less significant since the coolant flow in the manifolds is rather high and the value of the heat transfer coefficient is larger than that used above.

---

[1] *Alexi Radovinsky, Joule Heating of GEM Detector Bobbins, MIT-GEM-EM-014, (internal report), December 1992.*

[2] *Alexi Radovinsky, Joule Heating of GEM Detector Bobbin Cooling Tubes, MIT-GEM-EM-016, (internal report), March 1993.*

[3] *EDDYCUFF User's Manual ... (To be published)*

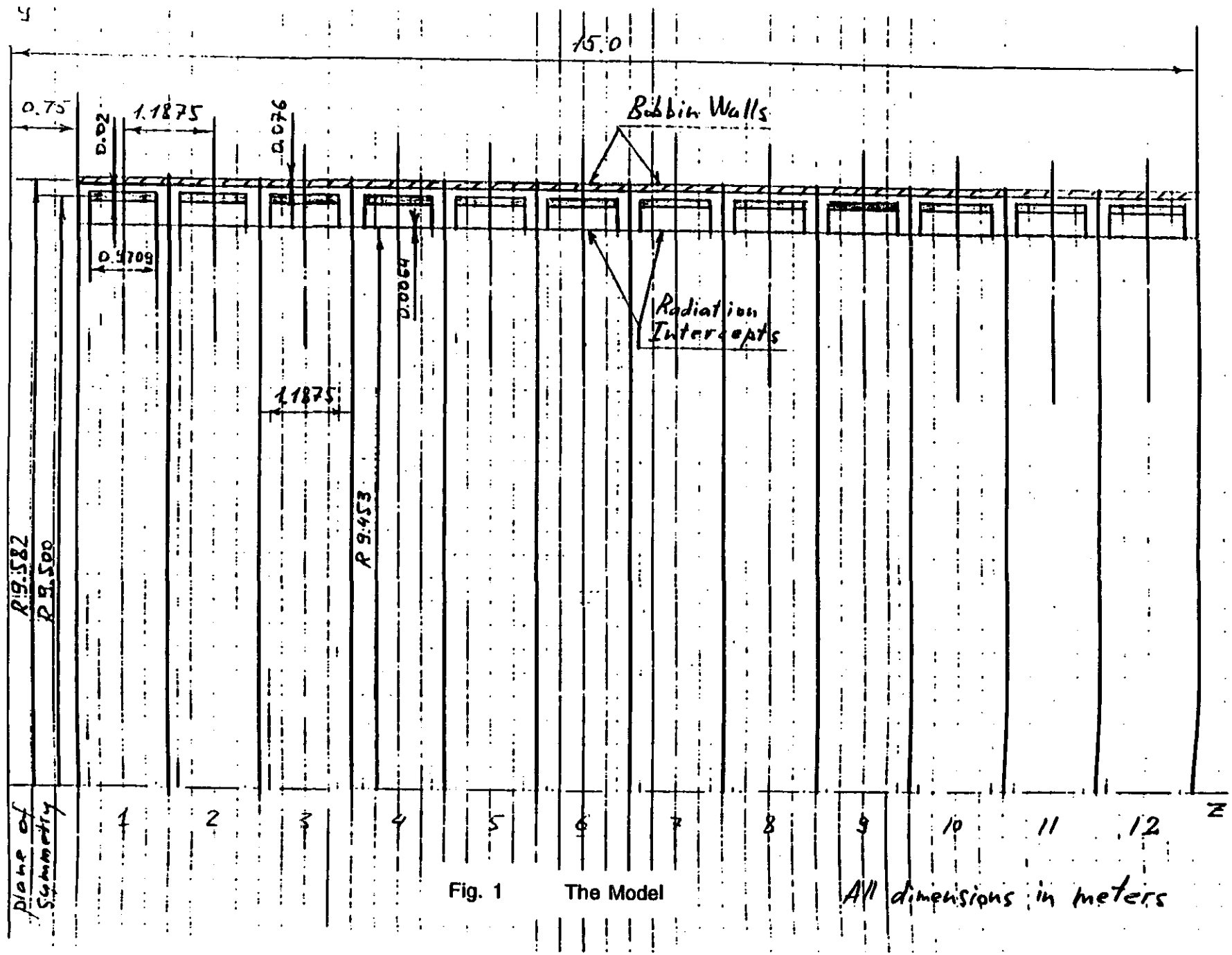

Fig. 1 The Model

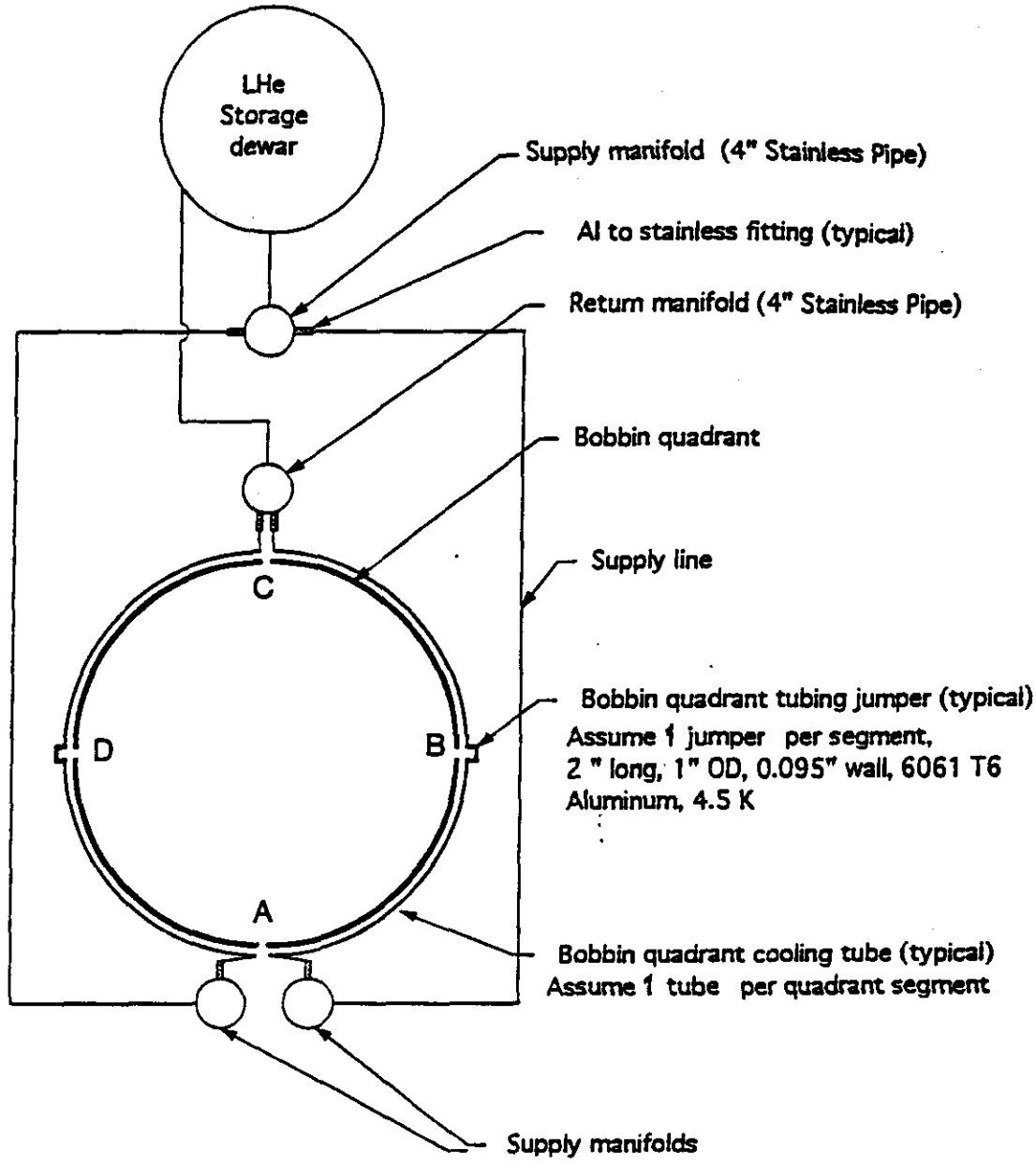

Fig. 2 Thermosiphon Plumbing Diagram

BAS
2/9/93

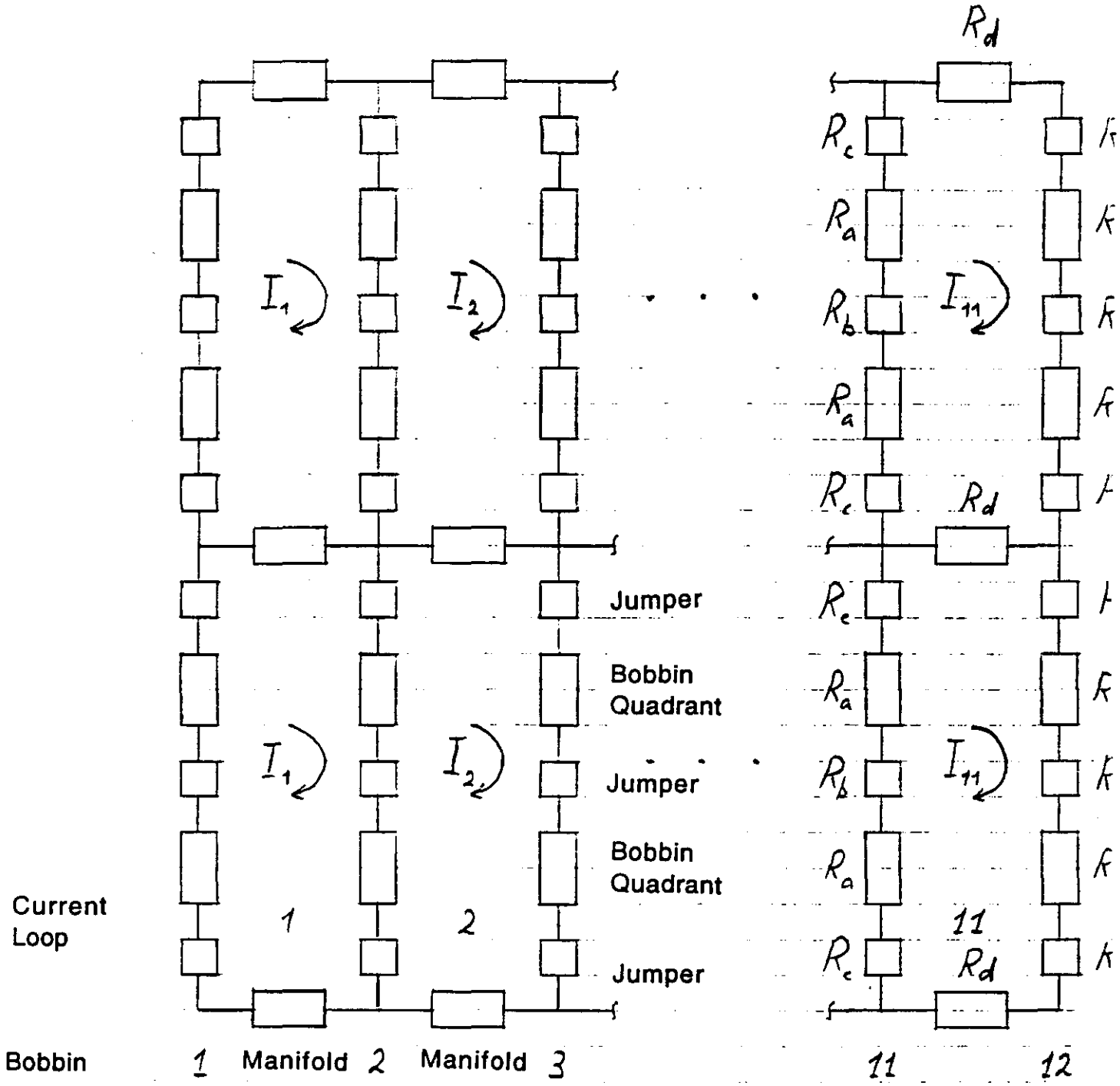

Fig. 3 Thermosiphon Electrical Model

Table 1. Resistances of the Circuit Elements

Part	Code	Material	Section area, m2	Length, m	Resistivity, Ohm*m	Resistance, Ohm
Quadrant	a	Al 6061	1.16E-01	15.0500	1.40E-08	1.82E-06
Quadrant to quadrant jumper	b	Al 1100	1.94E-04	0.0508	2.00E-09	5.24E-07
Quadrant to manifold jumper	c	Al 1100	1.94E-04	0.1000	2.00E-09	1.03E-06
Manifold	d	SS 304 L	1.92E-03	1.1875	4.90E-07	3.03E-04

Fig. 4 Radial component of B-field at R=9.582 m at t=0 s.

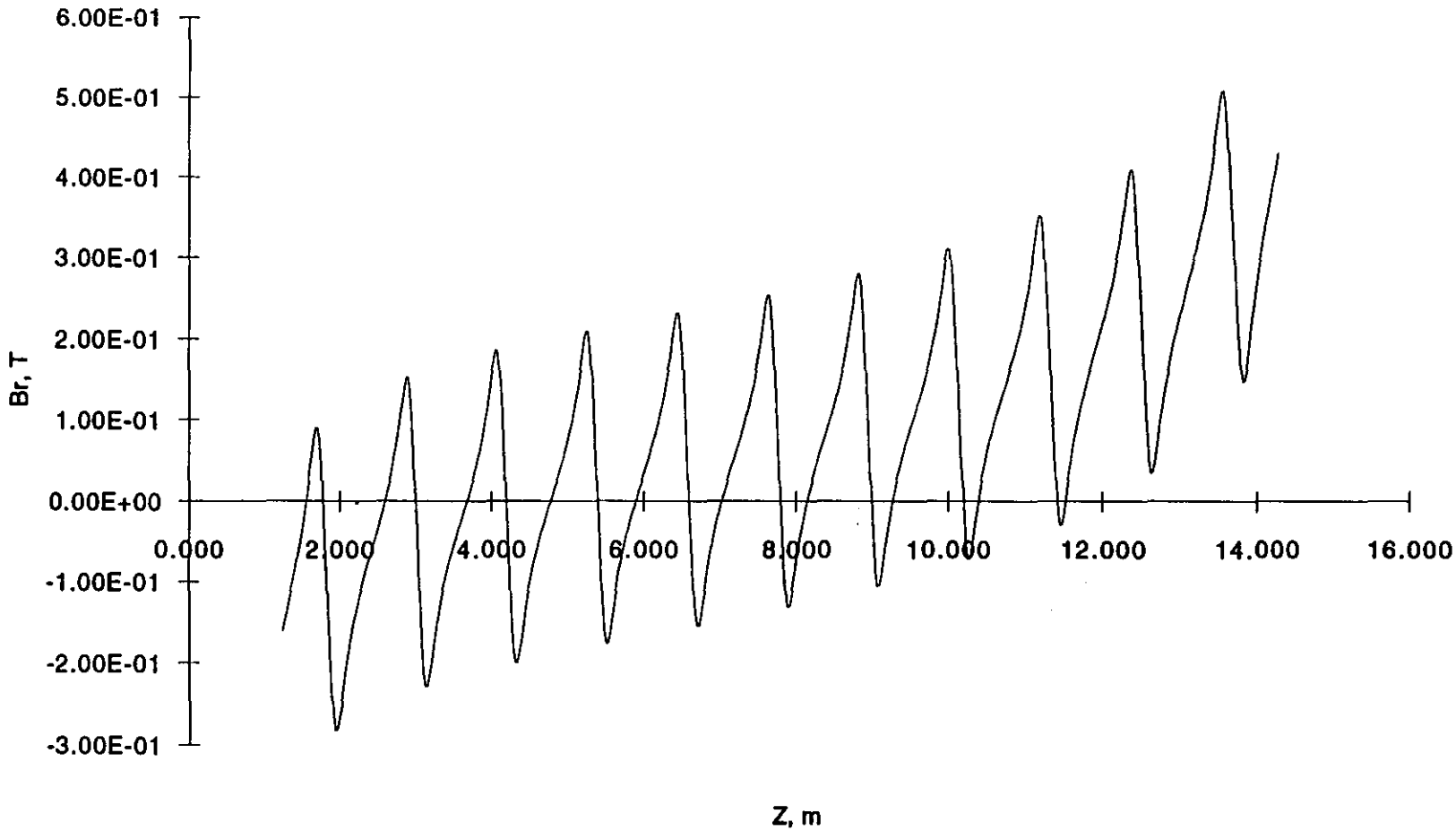

Table 2. Results of the Thermoelectrical Analyses

loop	Aver.Br, T	dFi/dt(0), V	Curr.I(0), A	mani.j(0), A/m2	mani.dT, K		bobin	Curr.I(0), A	jump.j(0), A/m2	jump.dT, K
1	-1.01E-01	-3.60E-02	-115.22	-6.00E+04	0.00354		1	-115.22	-5.94E+05	0.00056
2	-3.91E-02	-1.40E-02	-46.82	-2.44E+04	0.00058		2	68.39	3.53E+05	0.00020
3	-7.17E-03	-2.56E-03	-8.66	-4.51E+03	0.00002		3	38.16	1.97E+05	0.00006
4	1.69E-02	6.05E-03	19.95	1.04E+04	0.00011		4	28.61	1.47E+05	0.00003
5	3.90E-02	1.39E-02	46.10	2.40E+04	0.00057		5	26.16	1.35E+05	0.00003
6	6.19E-02	2.21E-02	73.27	3.82E+04	0.00143		6	27.16	1.40E+05	0.00003
7	8.80E-02	3.15E-02	104.17	5.43E+04	0.00289		7	30.90	1.59E+05	0.00004
8	1.20E-01	4.29E-02	142.08	7.40E+04	0.00538		8	37.90	1.95E+05	0.00006
9	1.62E-01	5.80E-02	192.18	1.00E+05	0.00985		9	50.11	2.58E+05	0.00011
10	2.24E-01	8.00E-02	265.50	1.38E+05	0.01880		10	73.32	3.78E+05	0.00023
11	3.35E-01	1.20E-01	385.13	2.01E+05	0.03956		11	119.62	6.17E+05	0.00061
							12	385.13	1.99E+06	0.00631